Open

Citation: J Sci Discov (2020); 4(2):jsd20029; DOI:10.24262/jsd.4.2.20029

Research Article

Fabrication of functionalized, low molecular weight (LMW) liquid crystalline nanoparticles: microstructures and thermal characteristics

Frank O. Ohwoavworhua[1,2,*] and James W. Mitchell[2]

[1]*Department of Pharmaceutical Sciences, College of Pharmacy, Howard University, Washington DC, USA*

[2]*Department of Chemical and Biomolecular Engineering, College of Engineering and Architecture, Howard University, Washington DC, USA*

Abstract Most research investigations continue to document the utilities of polymeric nanoparticles in drug delivery; however, a large number of these investigations are still at developmental and preclinical stages. Needed advancements for optimizing the benefits of polymeric nanoparticles for drug delivery include enhancing their multifunctional capabilities and the use of lower molecular weight nanomaterials. It is against this background that a low molecular weight, pH-responsive and functionalized liquid crystalline nanoparticles (LCNPs) was synthesized. LCNP was further assessed for average molecular weight, particulate and thermal characteristics. The average molecular weight is < 800 as determined by gel permeation chromatography (GPC), and the Raman spectrum shows that LCNP is bi-functionalized with C=C and COOH groups. The nanoparticles, which are hexagonal shapes, had average diameters of 307 nm and a zeta potential of – 53 mV; and an onset of thermal degradation of 204°C, with a glass transition and melting temperatures of 25°C and 315°C, respectively. We believe that a highly facile process, requiring few reactants, rather than a "cocktail" of compounds, has been developed for the synthesis of functionalized, low molecular weight LCNPs. The use of a few generally regarded as safe (GRAS) reagents, should make this technology a viable candidate for further development.

Keywords: Nanoparticles, pH-responsive, Low molecular weight,Liquid crystalline nanoparticles, ring-opening-dispersion-polymerization, thermal properties, zeta potential.

How to cite: Ohwoavworhua FO et al., Fabrication of functionalized, low molecular weight (LMW) liquid crystalline nanoparticles: microstructures and thermal characteristics. J Sci Discov (2020); 4(2):jsd20029; DOI:10.24262/jsd.4.2.20029; Received July 25th,2020, Revised August 21st ,2020, Accepted September 15th, 2020,Published September 21st, 2020.

Introduction

Nanoparticulate delivery systems have been investigated extensively for enhancing the ability to use poorly water-soluble or relatively unstable drugs/bioactive agents for practical applications (Elzoghby et al., 2012; Rao and Geckeler, 2011). In general, nanocarriers may protect a drug from degradation, enhance its absorption by facilitated diffusion through the epithelium, modify pharmacokinetics, enhance drug tissue distribution profiles, and/or improve intracellular penetration and distribution. In addition, by modulating the surface properties, composition and physicochemical environment of the drug, the desired drug release pattern and distribution can be achieved (Elzoghby et al., 2012; Firer and Gellerman, 2012; Danhier et al., 2010). Furthermore, nanoparticle formulations may reduce side effects and improve efficacy because nanoparticles can be designed to target drugs to different parts of the body where they are needed (Scot et al., 2012; Arias, 2011; Hall et al., 2007). Additionally, nanoparticles

* Correspondence: Dr. Frank O. Ohwoavworhua, Department of Chemical and Biomolecular Engineering, College of Engineering and Architecture, Howard University, Washington DC, USA. Email: frankohwo@gmail.com.

can serve as scaffolds for the attachment of chemical moieties that perform a variety of medical functions. For example, ligands for particular receptors can be attached to nanoparticles for "active targeting" to tissues expressing those receptors (Hughes, 2010; Hall et al., 2007; Wu et al., 2006; Allen, 2002). Thus, research to engineer nanoparticles, with the ability to combine several beneficial multifunctional features, continues to be extremely important.

Different types of nano-sized carriers, such as liposomes, solid lipid nanoparticles, ceramic nanoparticles, nanocrystals, magnetic nanoparticles, nanotubes, nanowires, nanocages, and polymeric nanoparticles (including dendrimers, micelles, polymer-drug conjugates, and liquid crystalline nanoparticles) are being developed for various drug-delivery applications (Hall et al., 2007; Rao and Geckeler, 2011). The polymeric nanoparticles can be fabricated from natural (including polysaccharides and proteins) and synthetic polymers.

Although research on the use of polymeric nanoparticles in drug delivery is extensive, most research work is still at developmental and preclinical stages (Perez-Herrero and Fernandez-Medarde, 2015; Narvekar et al., 2014; Lammers et al., 2012). Needed advancement for optimizing the benefits of polymeric nanoparticles for drug delivery include enhancing their multifunctional capabilities and the use of lower molecular weight nanomaterials. The latter will facilitate the ability of nanoparticles to direct drugs to target tissues across the mucosal membrane and/or via systemic circulation, and reduce induction of immunogenic responses (Narvekar et al., 2014; Li et al., 2004).

Low molecular weight substances, including polymers, have been correlated with increased permeability across epithelial cell membranes. For instance, it has been noted in transdermermal passage of uncharged molecules that the doubling of molecular weight from 400 to 800 g/mol for molecules, with the same lipophilicity, decreases permeability by a factor of almost 300-fold (Tozer and Rowland, 2006). In addition, the association between permeability and molecular weight of compounds was clearly demonstrated in a landmark investigation of Loehry et al., (1970). These investigators studied the intestinal permeability of substances of different molecular weight, ranging from 60–33,000. They observed an inverse relationship between permeability and molecular weight, and concluded that as the size of the molecule increases permeability drops considerably.

Further evidence supports the increased permeability of nanoconstructs in relation to low molecular weight of polymers (Zabaleta et al., 2012; Sahu et al., 2011; Xiao et al., 2014; Charlton et al., 2007). Zabaleta and co-workers (2012) reported the use of pegylated poly (anhydride) nanoparticles for oral administration of paclitaxel. The pegylation of the nanoparticles were achieved using three different poly (ethylene glycols) PEG: PEG 2000 (PTX-NP2), PEG 6000 (PTX-NP6) and PEG 10,000 (PTX-NP10). They found increased intestinal permeability of paclitaxel through the jejunum, compared with the commercial formulation, Taxol®. Also, they noted that the permeability was significantly higher for low molecular weight nanoconstructs (PTX-NP2 > PTX-NP6 > PTX-NP10), and the calculated relative bioavailability of paclitaxel, delivered in the nanoparticles, was 70%, 40% and 16%, respectively. Furthermore, Ghosh and Pramanik (2010) in an excellent review on the role of low molecular weight biodegradable polymer based nanoparticles, summarized that they are becoming very popular in delivery of nucleic acids, proteins and drugs. The current

interest in them results from their smaller particle size, higher solubilization ability, higher permeability, better biodegradability, high release efficiency, non-hemolytic nature, and low cytotoxicity at normal physiological conditions.

Considering the evidence provided above that correlates increased intestinal permeability to low molecular weight of polymeric nanomaterials, it would be beneficial to develop new processes for preparing low molecular weight nanoconstructs with capabilities of several beneficial features. More recently, liquid crystalline nanoparticle systems have been recognized as a versatile nanotechnology tool for the delivery of lipophilic, hydrophilic and amphiphilic drugs (Varma and Ahuja, 2016; Bu et al., 2015; Parmar et al., 2015; Li et al., 2015; Avachat and Parpani, 2014; Thanki et al., 2013; Zeng et al., 2012). The LCNPs, in comparison to other drug delivery systems, particularly the lipid-based system, have many advantages. The amphiphilic nature of the LCNPs, powerful solubilization, as well as high relative specific surface area properties, make them excellent carriers for a wide range of drugs. Also, their high compatibility with biological membranes, and adhesives properties make them suitable for use for application such as mucosal, parenteral, or topical delivery. Additionally, they have inherent ability to function as a sustained release matrix. These attributes accommodate their functions as versatile vehicle for delivery of drugs, and provide the rationale for our investigation. Thus, this paper reports the microstructures and thermal properties of a low molecular weight, functionalized LCNP.

Experimental

Materials

L-lactide (Polyscience Inc.) was recrystallized twice with toluene before use.

Toluene (Acros, 99%) was purified by drying over CaH_2 to remove moisture and oxygen and distilled under reduced nitrogen atmosphere. Hydroxyethyl methacrylate (HEMA) (Aldrich, 97%) was dried over molecular sieves (4 A°) for 24 hours and distilled under negative pressure before use. Stannous octoacte (Sigma, 95%) and phosphorous pentaoxide (Aldrich, 97%) were used as received. All other reagents were of analytical grade and used without further purification.

Synthesis of LMW Copolymeric Liquid Crystalline Nanoparticles

A low molecular weight, pH-responsive and functionalized liquid crystalline nanoparticle system was prepared directly from the monomer, L-lactide and an initiator, HEMA in novel ring-opening-dispersion-polymerization reaction. The reaction was carried out in the presence of 4-tert-butylcatechol (TBC), and stannous octoate, as a catalyst, using a published method (Huang and Onyari, 1996; Adesina and Akala, 2012), with slight modifications. Briefly, L-lactide (6.0234 g, 0.0418 mole), HEMA (5.0689 mL, 0.0418 mole), 4-tert-butylcatechol (347.32 mg) and drops of stannous octoate were placed in a 100 mL round-bottom flask equipped with a magnetic stirring bar. The reaction flask was kept under vacuum for 10 minutes and polymerization was carried out in an inert atmosphere by flushing the flask with nitrogen gas for 24 hours while heating from a silicone oil bath kept at 98 -102^{o}C. After polymerization was completed, the product (nanoparticles of PLA-HEMA i.e. co-polymeric nanoparticles) was purified.

Purification of Nanoparticles

The synthesized nanoparticles were purified and freed from unreacted reagents by rinsing in water thrice, followed by stirring the nanoparticles in excess water overnight. The copolymeric (actually oligomeric, since the average molecular weight as determined by GPC is less than 800, but for 'correctness' of terminology with respect to polymerization reaction, we have adopted copolymeric going forward) nanoparticles were collected by filtration and dried at room temperature in a vacuum desiccator under reduced pressure over phosphorous pentaoxide for 72 hours.

Melting Point, and Solution Characteristics

The melting point analysis was conducted using a Thomas® Hoover Unimelt^{TM} capillary melting point apparatus (Thomas Scientific, USA).

The behavior of the nanoparticles sample was estimated for its solution properties in different laboratory solvents including dilute alkaline solution, acetone, dilute hydrochloric acid, pyridine, methanol, ethanol, dimethyl sulfoxide (DMSO), triethylamine (TEA), tetrahydrofuran (THF), and chloroform.

Scanning Electron Microscopy

Dilute suspensions of the nanoparticles in different solvents were placed on a carbon tape affixed to a specimen steel stub (SPI Supplies, Inc) and dried for 24 hours in a vacuum oven. The samples were coated with gold for 2 minutes under argon atmosphere using a Hummer sputtering machine. The samples were then viewed under high vacuum at 10 kV and images taken at different magnifications using a scanning electron microscope.

Particle Size and Size Distribution Analysis

A 10 mg sample of desiccator-dried nanoparticles was dispersed in 5 mL of filtered distilled water using a probe sonicator at 30% amplitude for 120 seconds. The sonicated suspension was filtered through an Acrodisc® syringe filter with a 5 um Versapor® membrane (Pall Corporation, Port Washington, NY). The suspension was filled into a plastic cuvette and the particle size determined at 25 °C. Triplicate determinations were taken and the mean recorded. The polydispersity index (PI) provides information on the particle size distribution. The lower the value, the more uniform the nanoparticle size or the narrower the size distribution. This measurement and the zeta potential (described below) were executed by dynamic light scattering using a Zetasizer Nano-ZS (Malvern Instruments, USA).

Zeta Potential Determination

A 10 mg sample of desiccator-dried nanoparticles was dispersed in filtered distilled demineralized water using a probe sonicator as described for particle size analysis. By means of an Acrodisc® syringe filter equipped with a 5 μm Versapor® membrane (Pall Corporation), filtration was achieved. A 1.5 mL volume of the suspension was diluted with 2 mL of filtered distilled water and mixed by vortexing. The suspension was filled into a capillary zeta potential cell and analyzed. The measurement was carried out in triplicate and the mean recorded.

Contact Angle Measurement

The contact angle measurement was performed using Kruss G1 Goniometer (Kruss, Haburg, Germany) with MilliQ-Water (Millipore, Molsheim, France). This

instrument is equipped with a camera. Films of the nanoparticles from the suspension (15mg/10 mL methanol or acetone) were prepared on clean glass microscope slide cover slips. The films were dried under reduced pressure for 18 h prior to use. A syringe connected to a Teflon capillary of about 2 mm inner diameter was used to supply liquid (water) into the sessile drop from above. A sessile drop of about 0.4 – 0.5 cm radius was used. Once the drop was placed on the coated glass slide cover slip, then the drop is photographed. The photograph is processed and analyzed digitally by in-built machine software and two angles are measured, the left and right angles, and subsequently averaged. The above procedures were repeated for five drops on five new surfaces. All readings were then averaged to give an averaged contact angle. All experiments were performed at room temperature.

Gel Permeation Chromatography

The average molecular weight of the copolymeric LNCP was characterized by GPC (Waters 2690 separation modules). Waters 2410 differential refractive detector was used. PolyLab analytical column was used. The operating temperature for the column and detector was set at 35 °C. Tetrahydrofuran (THF), at a flow rate of 0.7 mL/min, was used as the eluent. The calibration of molecular weight was achieved by a series of polystyrene standard (PolyLab). The samples were prepared by dissolving the dried LNCP in THF at a concentration range of 0.1 – 0.2% and then filtered through a 0.45 um cellulose membrane filter.

FT-Raman Spectroscopic Measurement

FT-Raman spectrum was recorded with a FTS 100 FT Raman spectrometer (Brucker, Germany). An excitation wavelength at 1064 nm was provide by a cw Nd:YAG laser with a power of 200mW. All data were collected at a spectral resolution of 4 cm^{-1} from 3500 to 200 cm^{-1}. Four hundred scans were accumulated to ensure an acceptable signal-to-noise ratio, and it took about 10 min to record the FT-Raman spectrum.

Differential Scanning Calorimetry (DSC)

The DSC scans of the nanoparticle sample (5 mg) was recorded. Thermograms were obtained by heating from 5 to 500 °C at a heating rate of 10 °C/min under an inert nitrogen dynamic atmosphere (70 mL/min) in a sealed aluminum pan with the lid perforated, and an empty pan as a reference. The parameters obtained include glass transition (T_g) and melting point (T_m) temperatures.

Thermogravimetric Analysis

Thermogravimetric analysis was performed on a TA Instruments TGA Q50 thermogravimetric analyzer. The sample was analyzed in platinum pans at a heating rate of 10 °C/min to 750 °C in an atmosphere of air flowing at 60 mL/min, and the balance purge gas is nitrogen flowing at 40 mL/min. Sample masses ranged from 6-10 mg.

Results and discussion

Physicochemical Properties of LCNP

Table 1 presents results of some physicochemical properties for the copolymeric nanoparticle system. Two features are of interest. First, a clear solution is obtained when the nanoparticles sample was added to pyridine. Pyridine is an organic base. Thus, the complete dissolution of the product in pyridine indicates that it is an organic acid compound. The acid group was confirmed with the Raman spectrum. Secondly, strong hydration and gel-like

characteristic of the product in dilute sodium hydroxide. This property would contribute to the mucoadhesiveness of the material in the small intestine were the pH is alkaline. This has an important implication that would aid sustained drug delivery. Thus, the non-swelling characteristic in dilute hydrochloric acid and the observed considerable swelling - forming a gel-like mass – in dilute sodium hydroxide solution, demonstrates the pH-responsiveness of this LCNP system.

Table 1.Physicochemical Properties of Low Molecular Weight LCNPs

Melting Point (°C)	312 -328
Behavior in different solvents	
Sodium hydroxide (1&5%)	Strongly hydrated- forming gel mass
Hydrochloric acid (0.1N)	No appreciable effect
Pyridine	Forms a clear solution
Chloroform	Slightly solubilized
Tetrahydrofuran	Moderately solubilized, more on heating
Dimethylsulfoxide	Slightly solubilized

Scanning Electron Microscopy

The scanning electron micrographs of desiccator-dried nanoparticles are shown in Figures 1 – 2. Figure 1 represents the micrograph of the nanoparticles mounted from dilute alkaline solution (0.1 NaOH). They appear as flexible, highly aggregated, ball-like vesicles. The aggregation results from their tendency to form hydrated gel mass in alkaline solution. This morphology allows the nanoparticles to pass easily through a syringe. Such a system could result in possible broaden routes of drug administration, which may include injectables and peroral, if it is drug-loaded. The mean particle size of the nanoparticles, from the micrograph, approximates to 300 nm.

Figure 2 represents the photomicrograph of the nanoparticle system mounted from acetone. The hexagonal shaped discrete particles are revealed. This morphology is characteristic of liquid crystalline nanoparticles. Shapes of nanoparticles have been reported to play an important role in drug delivery, degradation, transport, targeting, and internalization (Lin et al., 2014). Champion and Mitragotri (2009) observed that the phagocytosis of drug delivery carriers through macrophages was found to be dependent on carrier shape. Also, Doshi et al., (2010) reported that modulating the shapes of drug–loaded nanoparticles controlled the flow and adhesion of drug delivery carrier throughout the circulatory system, and the *in vivo* circulation time of nanoparticles.

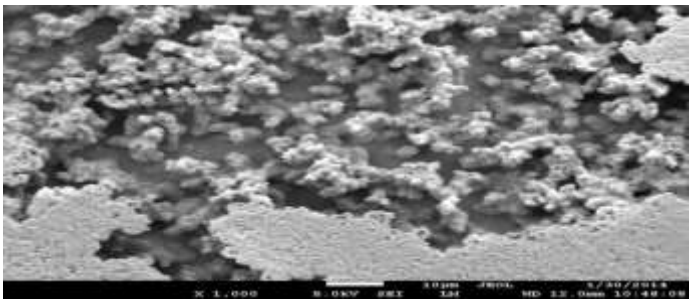

Size in µm

Figure 1: Scanning Electron Micrograph of the Copolymeric Liquid Crystalline Nanoparticles Showing Their "Ball-like" Vesicular Morphology when Mounted from Dilute Alkaline Solution

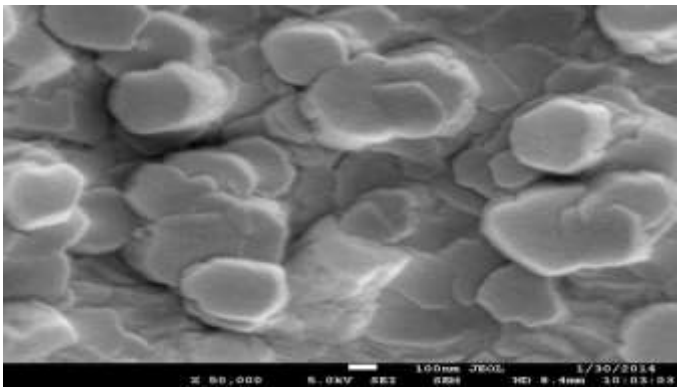

Size in nm

Figure 2: Scanning Electron Micrograph of the Copolymeric Liquid Crystalline
Nanoparticles Revealing the Hexagonal Morphology (Mounted from Acetone)

Particle Size and Size Distribution

The mean diameter of the particles is 307 nm, (Figure 3) and the polydispersity index (PI) is 0.3. The value of the PI indicates a fairly mono-dispersed narrow size distribution (Langer et al., 1996). PI value greater than 0.5 indicates broad size distributions (Langer et al., 1996). The pattern is consistent with mono-modal size distribution. The sizes of nanocarrier systems have been directly correlated with permeation abilities across physiological barriers. Jain (1987) reported that smaller systems translocate more rapidly from intravascular space to the interstitial space, and penetrate more readily through the interstitial space in a diffusion-driven transport. In addition, size plays a role in recognition of nanocarrier by the monocytes and the reticuloendothelial system (RES) of the body (Yokoyama, 1998). It is stated that a nanocarrier system with diameter larger than 200 nm (approximately) will induce nonspecific scavenging. The nanoparticle system obtained in this work has a mean particle size of 307 nm. Since this particle size is much larger than the pore size of renal filtration (which is approximately 8-12 nm), the copolymeric nanoparticle will evade renal excretion. The implication is that the nanoparticle will have a prolonged half-life and maintain stable circulation in the bloodstream. Hence, the size would undoubtedly play a significant role in determining the *in vivo* fate of the nanocarrier. Also, the size of the co-polymeric nanoparticles system would ideally allow extravasation from the bloodstream to target tissues (Yokoyama, 1998).

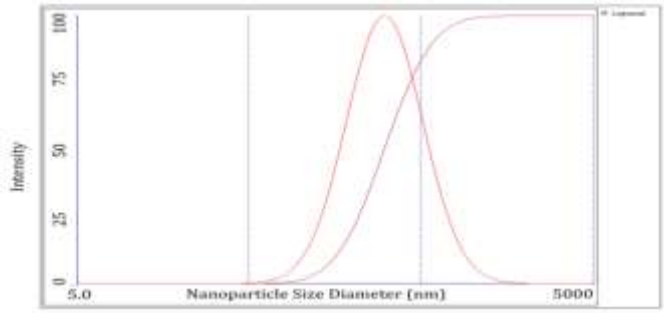

Figure 3: Particle Size Distribution of the Liquid Crystalline Nanoparticles.

Zeta Potential

The zeta potential of the copolymeric nanoparticle system was determined to be -53 mV at a pH of 7.4 (see Table 2). This high value is attributed to the strong dissociation of the carboxylic acid functional groups on the particles in an aqueous medium. Lukowski et al., (1992), in their work on characterization of surface properties relevant for *in vivo* organ distribution, explained that more negative surface charges on the copolymer nanoparticles lead to electrostatic repulsion between the polymerizing particles, resulting in decreased particle growth and a lower particle size. They also stated that development of electrostatic repulsion between the particles consequently results in high stability

for the colloidal suspension of this system. Other investigators stated that low zeta potential values result in colloidal instability, and may lead to aggregation (Freita and Muller, 1998, Clogston and Patri, 2011). Going further, the negatively charged nanoparticles should favor drug delivery, since they are not taken up by the reticuloendothelial system. Where the RES is the drug target, a positively charged nanocarrier system will lead to its high accumulation. This results from the electrostatic interactions, and hence their rapid adsorptions to the negatively charged cell membranes of the RES. In this respect, Nishida and co-worker (1990) showed, among other findings, that dextran of the same molecular weight (7,000), but different in positive and negative surface charges, were cleared at different rates in both the liver and kidney. An increased clearance with positive charges, and a decreased clearance with negative charges were observed. Takakura et al., (1994) similarly showed that unmodified bovine serum albumin (BSA), which is inherently negatively charged and 67,000 in molecular weight, has very slow clearance in both the liver and spleen. In contrast, with the introduction of positive charges, both the hepatic uptake and renal clearance were significantly enhanced. They noted that the enhancements in the clearance by an addition of positive charges might have resulted from electrostatic interaction between cationic macromolecules and anionic cell surfaces. Thus, surface charges of nanoparticles also influence the *in vivo* fate of the system.

Table2. Contact Angle and Zeta Potential Determinations

Determinations	Mean values
Contact angle (°)	56.9 ± 2.0
Zeta potential (mV)	- 53.0 ± 1.0

Contact Angle

The contact angle is the angle at which a liquid-vapor interface meets the solid surface. It measures the attraction of molecules within the droplet to each other versus the attraction or repulsion those droplet molecules experience toward the surface molecules (Zhang et al., 2009). It is a surface analysis technique and is often used to provide overall information about the hydrophobicity or the wettability/hydrophilicity of a surface (Temenoff and Mikos, 2008; Zhang et al., 2009). Hydrophilic surfaces have contact angles less than 90° while hydrophobic surfaces have angles greater than 90. Highly hydrophobic surfaces can be as high as 150° or even 180° (Zhang et al., 2009). Table 2 contains the contact angle value for the liquid crystalline nanoparticle system developed in this work. The value indicates that the surface of the nanoparticle system is hydrophilic in nature. This is expected since the surface of the nanoparticle (i.e. the outer shell) is carboxylic acid group functionalized. Also, the low value implies that the nanoparticle system will easily be wettable by physiological fluids and water, as well as implies that suspension of the nanoparticle system will easily be re-dispersible should sedimentation occurs during the course of use.

Gel permeation chromatography

The average molecular weight of LCNP as determined using GPC is about 724 as shown in Table 3 - thus, the copolymeric material that formed the nano-organogel by self-assembly has a low molecular weight. The importance of this in overall drug delivery are: (1) enhanced permeation of the nanocarriers across cell membranes, (2) little or no induction of immunogenicity and the decreased

tendency for the polymer to accumulate in the body, (Ghosh and Pramanik, 2010; Yokoyama, 1996).

Table 3. GPC Determination of Average Molecular Weight of LCNP

Mn	Mw	PI
627	724	1.16

Note: Mn is number average molecular weight; Mw is average molecular weight, and PI is polydispersity index.

FT-Raman Analysis

Figure 4 is the Raman spectrum of the nanoparticle system. The Raman spectroscopic study is a complementary technique to FT-IR. The spectrum shows a clear and defined peak at 1749 cm^{-1} due to stretching of C=O of an acid, as well as an O-H bend at 1384 cm^{-1}. The peak at 1641 cm^{-1} indicates the C=C vibration. Also, in the C-H stretching region a prominent band at 2946 cm^{-1} is observed. Thus, the carbonyl peak of an acid at 1749 cm^{-1} together with an O-H bend, and a C=C at 1641 cm^{-1} showed that LCNP is bi-functionalized.

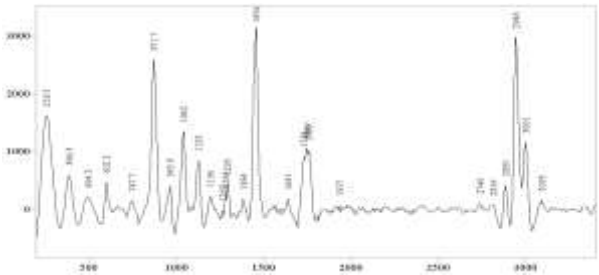

Figure 4: Raman Spectrum of the Copolymeric Liquid Crystalline Nanoparticles.

DSC Analysis

DSC is designed to measure endothermic and exothermic transitions as a function of temperature (Gabbott, 2008). The range of thermal events measured by this instrument includes melting, crystallization, glass transitions, curing reactions, and decomposition reactions. It finds popular use for characterizing polymers, metals, pharmaceuticals, organic, and inorganic compounds (Craig and Reading, 2007; Wunderlich, 2005). Figure 5 shows the DSC thermogram of a LCNP sample. Features of interest are two transition temperatures: glass transition temperature (Tg) at 25 °C and melting temperature (Tm) at 315 °C, corresponding to two thermal transitions: glass transition and melting peak, respectively. The values of Tg and Tm, when compared with values reported for previously synthesized PLA-HEMA copolymer, reveal that the LCNP system is formed from a novel PLA-HEMA copolymer. For instance, Huang and Onyari (1996) reported a Tg of 51 °C and a Tm of 167 °C for their synthesized PLA-HEMA copolymer.

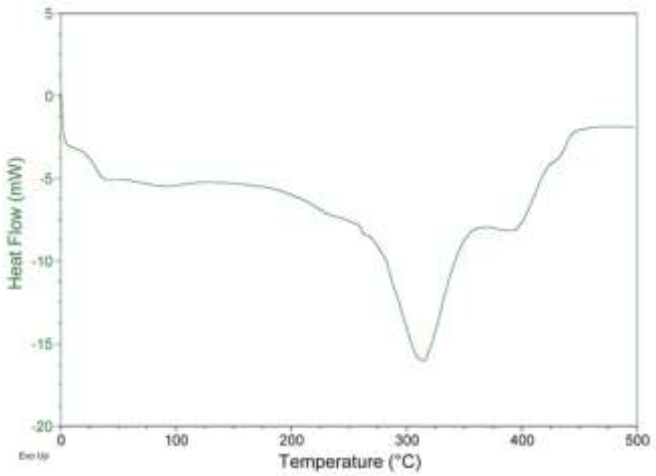

Figure 5: DSC Thermogram of the Copolymeric Liquid Crystalline Nanoparticles

The glass transition temperature (Tg) is an important characteristic property of amorphous polymers and/or amorphous regions of crystalline polymers (Zhang et al., 2009). Tg is a second order transition (has no peak), and is the critical temperature that delineates the glassy and rubbery behaviors of polymers (Zhang et al., 2009). In contrast, the melting transition, a first-order transition, is an

endothermic event because heat is required to break the fairly ordered crystalline structure in the solid state for the sample to become a disordered structure in the liquid state (i.e. melt). The melting peak of our nanoparticles is very broad, and this is expected since liquid crystalline nanoparticles have characteristically less ordered crystallites in their structure. Zhang et al., (2009) observed that very broad melting peaks are characteristics of semi-crystalline polymers whose different crystallites in the sample melt at different temperatures. All things taken together, our synthesized copolymer that self-assembled to form nanoparticles is composed of amorphous and semi-crystalline portions. The Tg and Tm determined for our nanoparticles have significant implications for both process and formulation scientists. The Tm being greater than 120 °C, coupled with the fact that the process for preparing these nanoparticles is surfactant-free, should make the nanoparticle system very readily amenable to further purification steps and sterilization processes, by autoclaving. For instance, heat sterilization by autoclaving may influence decomposition or degradation of active ingredient as well as nanoparticle materials. In this regards, Vauthier and Bouchemal (2008) reported that mechanical properties of polymers having melting points below 120 °C are strongly diminished after autoclaving. Also, another study showed that nanocapsule size increased from 200 to 500 nm after sterilization. The size increase was attributed to either swelling of polymeric membranes, which were composed of poly (Isobutyl cyanoacrylate) or expansion of the oily phase (Rollot et al., 1986). In addition, it was shown that autoclaving could catalyze some reactions with additives such as surfactants, which can modify the polymer constituting the nanoparticles (Masson et al., 1997). Thus, it should be emphasized that the surfactant-free synthetic reaction employed in the production of our nanoparticles adds to the novelty of the process.

TGA Analysis

The TGA analysis is widely used to characterize and verify the thermal behavior of materials. It finds application in various industries including pharmaceutical, food science, environmental and petrochemical (PerkinElmer). Figure 6 shows the TGA results generated from the co-polymeric liquid crystalline nanoparticle system. The plot shows the percent weight as a function of temperature of the nanoparticle sample under a nitrogen purge. The thermal curve shows that the nanoparticle sample undergoes thermal degradation beginning at 203.9 °C – corresponding to the onset temperature. For polymeric materials, onset temperature indicates its thermal stability. This value is important as it provides the information on the highest temperature that the nanomaterial can be subjected to during drug formulation processes (Zhang et al., 2009). In addition, the curve indicates that a weight loss has occurred. Also of note, is the point where the descending curve intercepts the abscissa at about 515 °C, while the percent weight axis is zero. This point indicates that the nanoparticle system is composed of 100% organic materials.

Furthermore, the thermal curve reveals that the nanoparticle sample decomposed in two steps; first rapidly, then slowly in a less steep slope over a temperature range of 420 °C to 520 °C. The two-step decomposition curve indicates that the nanomaterial from which the particles are fabricated is a copolymer. This determination using standard TGA could not, however, confirm the percent compositions of the copolymer. Such capability is only

possible with auto stepwise TGA determination (PerkinElmer).

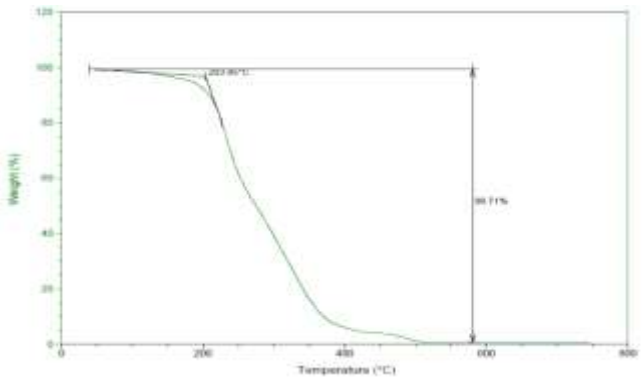

Figure 6: TGA Curve of the Copolymeric Liquid Crystalline Nanoparticles

Conclusion

It is concluded that a highly facile process, requiring few reactants, rather than a "cocktail" of compounds, has been developed for the synthesis of low molecular weight LCNPs. The bi-functionalization of LCNP will provide points of attachment for ligands to enhance its multifunctional capabilities. In addition, the use of a few generally regarded as safe (GRAS) reagents, should make this technology a viable candidate for further development.

Author Contributions

*Frank O. Ohwoavworhua (corresponding author: **frankohwo@gmail.com)** carried out the experimental synthesis and characterizations, as well as wrote the main manuscript. James W. Mitchell supervised the work. Both authors reviewed the manuscript.

Competing interests

The authors declare no competing interests

Funding Source Acknowledgement

None

References

1. Adesina SK, Akala EO. Biodegradable stealth polymeric particles fabricated using the macromonomer approach by free radical dispersion polymerization. US Patent 2012/0129797 A1.
2. Allen MT. Ligand-targeted therapeutics in anticancer therapy. Nat Rev Cancer 2002; 2:750-763.
3. Arias JL. Drug targeting strategies in cancer treatment: an overview. Mini Rev Med Chem 2011; 11:1-17.
4. Avachat AM, Parpani SS. Formulation and development of bicontinuous nanostructured liquid crystalline particles of efavirenz. Colloids Surf B Biointerfaces 2015; 126:87-97.
5. Bu M, Tang J, Wei Y, Sun Y, Wang X, Wu L, Liu H. Enhanced bioavailability of nerve growth factor with phytantriol lipid-based crystalline nanoparticles in cochlea. Int J Nanomedicine 2015; 3(10):6879-6889.
6. Champion JA, Mitragotri S. Shape induced inhibition of phagocytosis of polymeric nanoparticles. Pharm Res 2009; 26:244-249.
7. Charlton ST, Davis SS, Illum L. Evaluation of bioadhesive polymers as drug delivery systems for nose to brain delivery: in vitro characterization studies. J Control Release 2007; 118 (2):225-234.
8. Clogston JD, Patri AK. Zeta potential measurement. In: McNeil S. (eds) Characterization of Nanoparticles Intended for Drug Delivery. Methods in Molecular Biology (Methods and Protocols) vol 697. Humana Press 2011.
9. Craig DQM, Reading M. Thermal Analysis of Pharmaceuticals. FL, Boca Raton: CRC Press. 2007; 155-182p.
10. Danhier F, Feron O, Preat V. To exploit the tumor microenvironment: passive and active tumor targeting of nanocarriers for anti-cacer drug delivery. J Control Release 2010; 148: 135-146.
11. Doshi N, Prabhakarpandian B, Rea-Ramsey A, Pant K, Sundaram S, Mitragotri S. Flow and adhesion of drug carriers in blood vessel depend on their shape: a study model synthetic microvascular networks. J Control Release 2010; 146:196-200.

12. Elzoghby OA, Samy MW, Elgindy AN. Albumin-based nanoparticles as potential controlled release drug delivery systems. J Control Release 2012; 157: 168-182.
13. Firer M, Gellerman G. Targeted drug delivery for cancer therapy: the other side of antibodies. J Hematol Oncol 2012; 5:1-16.
14. Freita C and Muller RH. Effect of light and temperature on zeta potential and physical stability in solid lipid nanoparticles (SLN^{TM}) dispersions. Int J Pharmaceutics, 1998, 168(2), 221-229.
15. Gabbott P. Principles and Applications of Thermal Analysis. UK, Oxford: Blackwell Publishing 2008; 1p.
16. Ghosh D, Pramanik P. Low molecular weight biodegradable polymer based nanoparticles as potential delivery systems for therapeutics: The way forward? IJPSDR 2010; 2(1):31-34.
17. Hall BJ, Dobrovolskaia AM, Patri KA, McNeil ES. Characterization of nanoparticles for therapeutics. Nanomedicine 2007; 2(6):789-803.
18. Huang S, Onyari JM. Multicomponent polymers poly (lactic acid) macromonomers with methacrylate terminal and copolymers of poly (2-hydroxyethyl methacrylate). JMS Pure Appl Chem 1996; A33: 571-584.
19. Hughes B. Antibody-drug conjugates for cancer: poised to deliver? Nat Rev Drug Discov 2010; 9:665-667.
20. Jain KR. Transport of molecules across tumor vasculature. Cancer and Metastasis Reviews 1987; 6:559-593.
21. Lammers T, Kiessling F, Hennink WE, Storm G. Drug targeting to tumors: principles, pitfalls and (pre-) clinical progress. J Control Release 2012; 161:175-187.
22. Langer K, Marburger C, Berthold A, Kreuter J, Stieneker F. Methylmethacrylate sulfopropylmethacrylate copolymer nanoparticles for drug delivery. Part 1: preparation and physicochemical characterization. Int J Pharm 1996; 137:67-74.
23. Li ZZ, Wen LX, Shao L, Chen JF. Fabrication of hollow silica nanoparticles and their applications in drug release control. J Control Release 2004; 98: 245-254.
24. Li JC, Zhu N, Zhu JX, Zhang WJ, Zhang HM,Wang QQ, Wu XX, Wang X, Zhang J, Hao JF. Self-assembled cubic liquid crystalline nanoparticles for transdermal delivery of Paeonol. Med Sci Monit 2015; 21:3298-3310.
25. Lin P-C, Lin S, Wang PC, Sridhar R. Techniques for physicochemical characterization of nanomaterials. Biotechnol Adv 2014; 32(4): 711-726.
26. Loehry CA, Axon TRA, Hilton JP, Hider CR, Creamer B. Permeability of the small intestine to substances of different molecular weights. Gut 1970; 11: 466-470.
27. Lukowski G, Muller RH, Muller BW, Dittgen M. Acrylic acid copolymer nanoparticles for drug delivery: 1. Characterization of the surface properties relevant for *in vivo* organ distribution. Int J Pharm. 1992; 84: 23-31.
28. Masson V, Maurin F, Fessi H, Devissaguet JP. Influence of sterilization processes on poly (ε-caprolactone) nanospheres. Biomaterials 1997; 18:327-335.
29. Narvekar M, Xue HY, Eoh JY, Wong HL. Nanocarrier for poorly water-soluble anticancer drugs – barriers for translation and solutions. AAPS PharmSciTech. 2014; 15(4): 822-833.
30. Nishida K, Tonegawa C, Nakane S, Takakura Y, Hashida M, Sezaki H. Effect of electric charge of the hepatic uptake of macromolecules in the rat liver. Int J Pharm. 1990; 65:7-17.
31. Parmar R, Misra R, Mohanty S. *In vitro* release of Rifampicin through liquid-crystalline folate nanoparticles. Colloids Surf B Biointerfaces. 2015; 129: 198-205.
32. Perez-Herrero E, Fernandez-Medarde A. Advanced targeted therapies in cancer: Drug nanocarriers, the future of chemotherapy. Euro J Pharmaceut Biopharm 2015; 93: 52-79.
33. Pruckmayr G, Dreyfuss P, Dreyfuss MP. Polyethers, tetrahydrofuran and oxetane polymers, In: Kirk-Othmer Encyclopedia of Chemical Technology. John Wiley & Son, Inc. 1996.
34. Rao JP, Geckeler EK. Polymer nanoparticles: Preparation techniques and size-control parameters. Prog Polym Sci. 2011; 36: 887-913.
35. Rollot J, Couvreur P, Roblot-Treupel L, Puisieux F. Physicochemical and morphological characterization of polyisobutylcyanoacrylate nanocapsules. J Pharm Sci. 1986; 75:361-364.
36. Sahu A, Kasoju N, Gosawami P, Bora U. Encapsulation of curcumin in pluronic block copolymer micelles for drug delivery applications. J Biomater Appl. 2011; 25: 619-639.
37. Scott AM, Wolchok DJ, Old JL. Antibody therapy of cancer. Nat Rev Cancer. 2012; 12: 278-287.
38. Takakura Y, Fujita T, Hashida M, Sezaki H. Disposition characteristics of macromolecules in tumor-bearing mice. Pharm Res. 1994; 7:339-346.
39. Temenoff JS, Mikos AG. Biomaterals: The Intersection of biology and material science. 1^{ST} Ed. New Jersey: Pearson Education Inc.2008; 249p.

40. Thanki K, Gangwal PR, Sangamwar TA, Jain S. Oral delivery of anticancer drugs: challenges and opportunities. J. Control Release 2013; 170:15-40.
41. Tozer NT, Rowland M. Introduction to Pharmacokinetics and Pharmacodynamics. MD, Baltimore: Lippincott Williams and Wilkins. 2006; 49p.
42. Varma P, Ahuja M. Cubic liquid crystalline nanoparticles: optimization and evaluation for ocular delivery of tropicamide. Drug Deliv. 2016; 15: 1-12.
43. Vauthier C and Bouchemal K. Methods for preparation and manufacture of polymeric nanoparticles. Pharm Res, 2009; 26:1025-1058.
44. Wu CH, Chang KD, Huang TC. Targeted therapy for cancer. J Cancer Mol. 2006; 2:57-66.
45. Wunderich B. Thermal Analysis of Polymeric Materials. Berlin Springer-Verlag. 2005; 1-58p.
46. Xiao Y, Li P, Cheng Y, Zhang X, Sheng J, Wang D, Li J, Zhang Q, Zhong C, Cao R, Wang F. Enhancing the intestinal absorption of low molecular weight chondroitin sulfate by conjugation with α-linolenic acid and the transport mechanism of the conjugates. Int J Pharm. 2014; 465(1-2):143-158.
47. Yokoyama M. Novel passive targetable drug delivery with polymeric micelles. In: Okano T (ed), Biorelated Polymers and Gels: Controlled Release and Application in Biomedical Engineering. UK, London: Academic Press.1998.
48. Zabaleta V, Ponchel G, Salman H, Agueros M, Vauthier C and Irache JM. Oral administration of paclitaxel with PEGylated poly (anhydride) nanoparticles: Permeability and pharmacokinetics study. Eur J Pharm Biopharm 2012; 81: 514-523.
49. Zeng N, Gao X, Hu Q, Song Q, Xia H, Liu Z, Gu G, Jiang M, Pang Z, Chen H, Chen J, Fang L. Lipid-based liquid crystalline nanoparticles as oral drug delivery vehicles for poorly water-soluble drugs: cellular interaction and in vivo absorption. Int J Nanomedicine. 2012; 7: 3703-3718.
50. Zhang S, Li L, Kumar A. Materials Characterization Techniques. NY: CRC Press 2009.